Proceedings of the 16th International Conference on Soil Mechanics and Geotechnical Engineering

doi:10.3233/978-1-61499-656-9-1599

Unsaturated hydraulic properties for compressed air tunnelling by inverse modeling

Modélisation inverse des caractéristiques hydrauliques non saturées pour la construction de tunnel sous air comprimé

A. Chinkulkijniwat, S. Semprich, & G. Steger
Institute for Soil Mechanics and Foundation Engineering, Graz University of Technology, Austria

ABSTRACT

A large scale element test was carried out to determine the unsaturated hydraulic properties of silty sand. To simulate air flow likewise in compressed air tunnelling, where air pressure is used to prevent water inflow during excavation, air pressure was upward injected from the bottom part of a saturated soil column. A series of constant head permeability experiments were conducted before to derive the saturated hydraulic conductivity. Thereafter the transient flow experiments were performed. UCODE in combination with TOUGH2 was employed to estimate the unsaturated hydraulic properties. To check the uniqueness of the solution, response surfaces were plotted and analyzed. Finally the derived parameters were employed in a 3D-numerical tunnel advance simulation to calculate the rate of air flow, which is one determining cost factor in the compressed air tunnelling method. The results show a very good coincidence with a comparable tunnelling project carried out in Munich.

RÉSUMÉ

Un essai à grande échelle a été exécuté pour déterminer les caractéristiques hydrauliques non saturés d'un sable limoneux. l'écoulement de l'air dans l'essai est orienté de bas en haut, afin de reproduire les conditions dans la construction de tunnels sous air comprimé. Dans ces constructions l'air est utilisé pour éviter que l'eau de la nappe phréatique pénètre dans le tunnel. Une série d'essai de perméabilité à gradient hydraulique constant a été conduite antérieurement pour déterminer le coefficient de perméabilité. En suite des essais à écoulement non stationnaire ont était conduits. Les caractéristiques hydrauliques du milieu non saturés sont estimées à l'aide de UCODE en combinaison avec TOUGH2. Pour étudier la généralité de la solution les surfaces de réponses sont dessinées et analysées. Finalement, les paramètres estimés sont employés dans une simulation spatiale d'un avancement de tunnel sous air comprimé pour déterminer le volume d'air nécessaire. Le volume d'air nécessaire est un facteur important sur les coûts de construction. Les résultats de l'analyse montrent un bon accord avec un projet comparable exécuté à Munich.

1 INTRODUCTION

For shallow tunnelling below ground water table, the New Austrian Tunnelling Method (NATM) is frequently used in combination with compressed air. To prevent water inflow, the magnitude of the air pressure must be at least equal to the ground water pressure at the invert of the tunnel. The hydrostatic pressure distribution of the ground water and the constant head of air pressure over the height of the tunnel cause an unavoidable pressure difference, which has a maximum at the tunnel crown. This leads to an escape of air into the surrounding soil. The surrounding soil which is initially saturated will become unsaturated (Fig. 1). Due to the air flow, continual compensation is needed to keep the air pressure at the necessary level. The energy costs for generating the compressed air, may reach a significant factor of the total project costs.

A 3-D numerical program in TOUGH2 (Preuss et al., 1999) environment (Scheid 2003, Steger 2004) is employed to simulate the described two phase flow in compressed air tunnelling. Detailed knowledge of unsaturated hydraulic properties, including water retention curve and hydraulic conductivity curves are essential for reasonable results.

For the presented study, the unsaturated hydraulic properties of silty sand, whose particle size distribution shown in Fig. 2, are determined. Therefore a series of transient flow experiments in a large soil column were performed. The experimental results including cumulative water outflow, the changes of volumetric water content and of pressure levels were used for inverse modeling to estimate the required parameters.

Although inverse modeling has been widely used to determine unsaturated hydraulic properties for decades now, few of them were carried out as large scale element tests. Moreover, based on the authors' knowledge, none of those large scale element tests used air as an active phase, especially flowing in an upward direction.

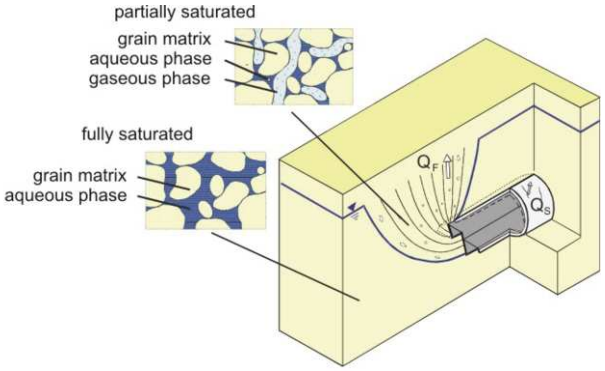

Figure 1. Two phase flow in compressed air NATM-tunnelling

2 MATERIAL AND EXPERIMENT

A large scale experiment for 1 dimensional transient outflow was carried out for the silty soil. To imitate flow like in compressed air tunnelling, air had to be injected in an upward direction. Experimental equipment was, therefore, decided to serve this purpose. A general layout of the experimental setup is shown in Fig. 3. It is also worth noting that a small surface load on top of the soil column was necessary to prevent failure of the

experiment due to the development of macro-pores and soil loosening close to the surface.

A Plexiglas cylinder having an inner diameter of d = 0.44 m was used to pack a soil column with a height of h = 0.45 m. The studied soil was oven dried under 70°C, sieved, and then packed into the Plexiglas cylinder, achieving a dry density of ρ_d = 1.54 ton/m^3. As the specific gravity of the soil grain is ρ_s = 2.74 g/cm^3, a porosity of n = 0.44 results for the soil. While packing the soil column, pressure gauges (P1 and P2) and TDR (time domain reflectory) probes (T1-T4) were installed to monitor the pressure head and the volumetric water content during the transient flow experiments.

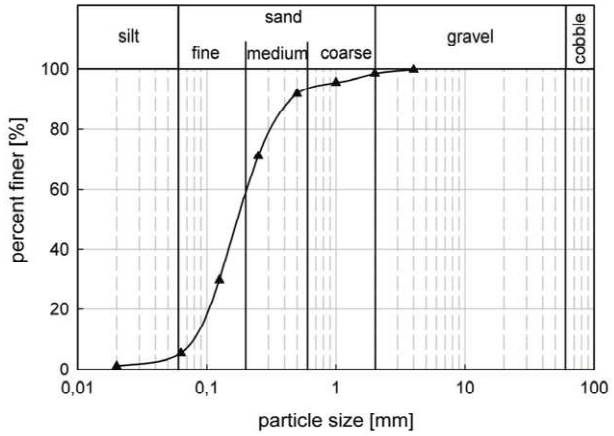

Figure 2. Particle size distribution of the studied soil

The homogeneity of the soil column was ensured by packing the soil by layers of 5 cm thickness and controlled by taking samples at three different heights and subsequent determination of their grain size distributions. Thereafter, a series of constant head permeability experiments were carried out from these samples. The intrinsic hydraulic conductivity was found of K = 7.7 x 10^{-12} m^2. It is noted that after performing each permeability experiment, a maximum liquid saturation of S_{ls} = 98% was found for the samples.

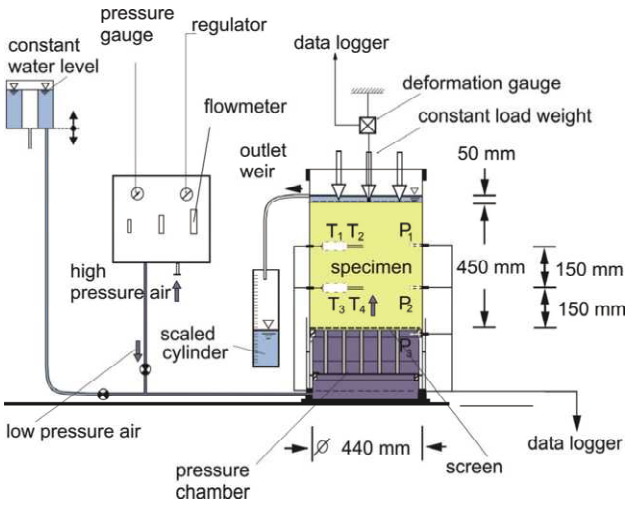

Figure 3. Layout of the transient outflow experiment

In the transient experiments, the soil column was saturated by stepwise raising the level of a water reservoir (see Fig. 3). Each step was hold until steady flow was reached. The last step, where the level of the water reservoir was at 0.05 m above the surface of the soil column, was hold for 24 hours. It was observed that the water table in the Plexiglas cylinder was also 0.05 m above the surface of the soil column. The pressure distribution read from the pressure gauges (P1 and P2) showed a hydrostatic pressure distribution. The volumetric water content, which was averaged from the measurements of the TDR probes (T1-T4), reached θ = 0.40. The measured liquid saturation and pressure distribution after saturation would be then used as initial conditions for a numerical simulation in the inverse modeling.

The transient flow experiment was then performed by stepwise increasing the magnitude of air pressure in the pressure chamber beneath the soil column. Fig 5b shows among others a graph with the magnitude of the applied air pressure versus time scale. During the experiment, the water outflow was collected via an outlet weir in a graduated cylinder and continuously recorded by an electrical balance. Meanwhile, the volumetric water content and the pressure inside the soil column were continuously recorded by a data logger which was connected to the TDR probes (T1-T4) and the pressure gauges (P1 and P2).

3 GOVERNING EQUATIONS AND CONSTITUTIVE MODELS

Considering the soil as a non deformable porous media the governing equation for transient flow derived by introducing an extended Darcy's law for unsaturated flow into the continuity equation reads:

$$\frac{D(nS_\alpha \rho_\alpha)}{Dt} = \mathbf{div}\left(\rho_\alpha \mathbf{K} \frac{k_\alpha(\theta)\rho_\alpha}{\mu_\alpha} (\nabla p_\alpha - \rho_\alpha \mathbf{g}) \right) \quad (1)$$

where a subscript α stands for liquid resp. gas phase, p_α denotes the pressure, S_α the degree of saturation, n the porosity of the porous medium and ρ_α the density. **K** is the intrinsic saturated hydraulic conductivity matrix, μ_α the viscosity, $k_\alpha(\theta)$ the relative hydraulic conductivity as a function of the volumetric water content, θ and **g** is the gravitational vector.

Additional constitutive equations for capillary pressure and relative hydraulic conductivity are needed to solve Eq. (1). In this paper, the van Genuchten model (van Genuchten, 1980) was used to represent the capillary pressure function whereas the van Genuchten-Mualem model (Mualem, 1976) was used to represent the relative hydraulic conductivity of the liquid phase. The Corey model (Corey, 1954) was used for the relative hydraulic conductivity of the gas phase.

The van Genuchten, van Genuchten-Mualem and Corey equations are written in Eq.(2), Eq. (3), and Eq. (4) respectively:

$$p_c = -p_o (S_e^{-1/m} - 1)^{1-m} \quad (2)$$

$$k_{rl} = S_e^\tau \{1 - (1 - S_e^{1/m})^m\}^2 \quad (3)$$
$$\text{and } S_e = (S_l - S_{lr})/(S_{ls} - S_{lr})$$

$$k_{rg} = (1 - \hat{S})^2 (1 - \hat{S}^2) \quad (4)$$
$$\text{and } \hat{S} = (S_l - S_{lr})/(1 - S_{lr} - S_{gr})$$

where p_c is the capillary pressure, p_o is the air entry pressure, m is the pore size distribution factor, k_{rl} is the relative hydraulic conductivity of liquid phase, k_{rg} is the relative hydraulic conductivity of gas phase and τ is the tortuosity factor. S_l denotes the liquid saturation, S_{lr} the residual liquid saturation, S_{ls} the maximum liquid saturation and S_{lr} is the residual gas saturation.

The numerical simulation of the experiment was performed under TOUGH2 environment. The initial conditions are what had been found from the laboratory, a volumetric water content of θ = 0.40 and a hydrostatic pressure distribution. At the top surface of the soil column a Dirichlet condition with a prescribed access pressure of 5 mbar was assigned. The pressure chamber beneath the soil column was also simulated by assigning a Dirichlet condition having a time dependent pressure state as shown in Fig. 5b.

4 OPTIMIZATION PRECEDURE

UCODE (Poeter and Hill, 1998) was employed to perform inverse modeling with the TOUGH2 simulation of the experiments. UCODE executes TOUGH2 iteratively to solve the governing equation expressed in Eq. (1). Each iteration, the estimated parameters are changed (perturbed) one by one to determine the parameter sensitivities to the model responses. The parameter sensitivities associated to the model residuals (e.g. the differences between the measurements and the model predictions) were then used to update a set of new estimated parameters for a next iteration. The differences between the measurements and the model predictions expressed in Eq. (5) were minimized using the Modified Guess-Newton (also called Levenberg-Marquart) optimization algorithm. The minimization process had to be performed until convergence was reached. In this paper, the convergence criteria were either the maximum change of a single parameter less than 2 percent or the change of the sum of square weighted residuals less than 2 percent.

$$O(\mathbf{b}) = \sum_{i=1}^{NQ} \{w_{qi}\left[Q(t_i) - Q'(t_i,\mathbf{b})\right]\}^2 + \sum_{j=1}^{NT} \{w_{\theta i}\left[\theta(t_j) - \theta'(t_j,\mathbf{b})\right]\}^2 + \sum_{k=1}^{NP} \{w_{pk}\left[P(t_k) - P'(t_k,\mathbf{b})\right]\}^2 \quad (5)$$

where O(b) is the objective function to be minimized, **b** denotes the vector containing a set of estimated parameters, NQ is the number of the measured cumulative water outflow, NT is the number of the measured volumetric water content, NP is the number of the measured pressure. The notation Q, θ and P denotes the measured cumulative water outflow, the measured volumetric water content at a mid level of the soil column, and the measured pressure at the observation point respectively. Whereas, same notations with prime (Q', θ' and P') denote those predicted from the model. The notation w_{mn} denotes weighting factors for quantity m at n^{th} measurement.

Due to an ease in determining, the intrinsic saturated hydraulic conductivity **K** and the maximum degree of liquid saturated S_{ls} were derived independently from the constant head permeability experiments. The values of these parameters are reported in section 2. Assuming that the maximum liquid saturation of the soil column is also the limit state for gas flow, the residual gas saturation therefore is S_{gr} = 2%.

5 EXPERIMENTAL RESULTS

Fig. 4 shows contour plots of the logarithm of the objective function O**(b)** on different pair of parameters to be estimated. These plots are commonly called response surfaces. In this paper, the response surfaces are used for checking the existence and uniqueness of the solution. If the response surfaces did not display a clear global minimum, failure of inverse problem would have to be expected. A clear global minimum of the objective function O**(b)** can be found in every plane of the estimated parameters. However, the response surfaces plotted in Fig. 4b, 4c and 4d with a $1/p_o$ axis exhibit a long narrow valley shape indicating a probably difficulty to solve the inverse problem. The direction of the valley is almost perpendicular to the $1/p_o$ axis which indicates that the uncertainty associated with the other estimated parameters is higher and, thus, more sensitivity of the objective function to the parameter p_o than to the other parameters.

However, the response surface plots on the other pairs of the estimated parameters show compact elliptical shapes (Fig. 4a, 4e, and 4f). Stable parameters as well as about equal sensitivity among these parameters are expected. As a result, experimental data from the laboratory contains sufficient information to estimate the four parameters m, τ, $1/p_o$ and S_{lr}.

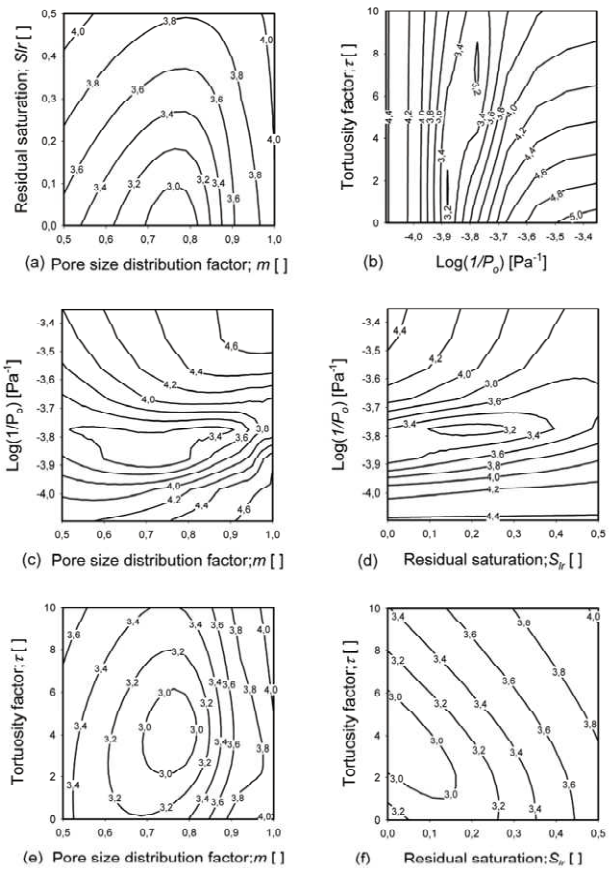

Figure 4. Response surfaces of the log of objective function

Table 1: Summary of hydraulic parameters of the studied soil

Parameter				
Fixed parameters				
Intrinsic hydraulic conductivity; **K** [x 10^{-12}m^2]				7.7
Maximum liquid saturation; S_{ls} [ ]				0.98
Residual gas saturation; S_{gr} [ ]				0.02
Estimated parameters				
Pore size distribution factor; m [ ]				0.77 (0.74-0.80)
Inverse of air entry pressure; $1/p_o$ [x 10^{-4} Pa^{-1}]				1.46 (1.40-1.53)
Residual saturation; S_{lr} [ ]				0.00 (0.00-0.00)
Tortuosity factor; τ [ ]				4.23 (2.72-5.73)
Correlation matrix				
	m	S_{lr}	$1/p_o$	τ
m	1.00	0.00	0.90	0.87
S_{lr}	0.00	1.00	0.00	0.00
$1/p_o$	0.90	0.00	1.00	0.94
τ	0.87	0.00	0.94	1.00

A summarization of the derived hydraulic parameters of the studied soil is given in Table 1. The values written in parenthesis represent a 95% confidence interval. A strong correlation can be found for the parameter pairs $1/p_o$ - τ, m - $1/p_o$ and τ - m. However, these correlations are still less than the critical value of 0.95 (Poeter and Hill, 1998), therefore the parameter correlations are not a problem. Fig. 5 shows a comparison between the measurements and the simulations of the cumulative water outflow from the soil column, the average volumetric water content and the average pressure at the middle part of the soil column. The coefficient of correlation between weighted simulation and weighted measurement is 0.987.

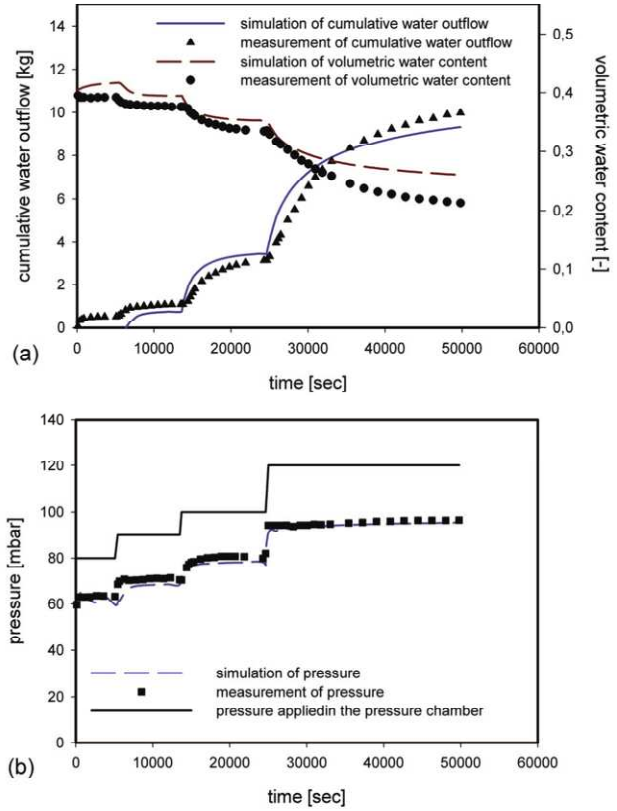

Figure 5. Comparison between experimental results and simulations

6 THREE DIMENSIONAL COMPRESSED AIR TUNNEL ADVANCE SIMULATION AND DISCUSSION

The derived hydraulic parameters for the studied soil were used to calculate the rate of air flow for a compressed air tunnelling problem. The geometry of the 3-D model is shown in Fig 6a. The advance simulation was performed with the program ASCATA (Steger 2004), which was developed in TOUGH2 environment. For the tunnel, having a diameter of d = 6.0 m, an advance of 45 m was simulated. The initial conditions for the soil were a liquid saturation of 100 % and a hydrostatical pressure distribution. A Neumann condition with zero flux was assigned at every boundary of the model except at the top surface, where a Dirichlet condition with atmospheric pressure was assigned.

The amount of air flow from the tunnel space is of interest in this paper. The air flow can take place both through the unsupported tunnel face and cracks along the shotcrete lining. Based on laboratory tests of Kammerer (2000), an intrinsic permeability of $7x10^{-14}$ m^2 was derived for the shotcrete lining. Additionally, a linear relative permeability functions for both, the gas and the liquid phase was prescribed. The speed of tunnel advance is 3 m/day. Full details on the three dimensional tunnel advance model are described in Steger (2004).

Fig. 6b shows graphs of the air flow from the tunnel into the surrounding soil. The air flow through the tunnel face reaches a constant value of 850 m^3/h after about 6 m of tunnel advance. The air flow through the shotcrete lining increases with a rate of 55 m^3/h per m of tunnel advance, what means an air flow of 0.05 m^3/min per m^2 shotcrete lining. This value coincides well with an observed air flow of 0.06 m^3/min per m^2 for a comparable tunnelling project carried out in Munich (Arz et al. 1994). After 45 meter of tunnel advance, the total rate of air flow is 3200 m^3/h. The jumps in the graphs origin from the discretization of the tunnel advance in 2 m round lengths.

The simulation results shown in Fig. 6b are based on the assumption, that the air and liquid flow take place through the soil in a homogenous way. However, the development of macropores, which can be observed at higher pressure levels was not considered in the study. This phenomenon might lead to a higher air flow than evaluated with the employed model. Further experimental research on this special topic is necessary.

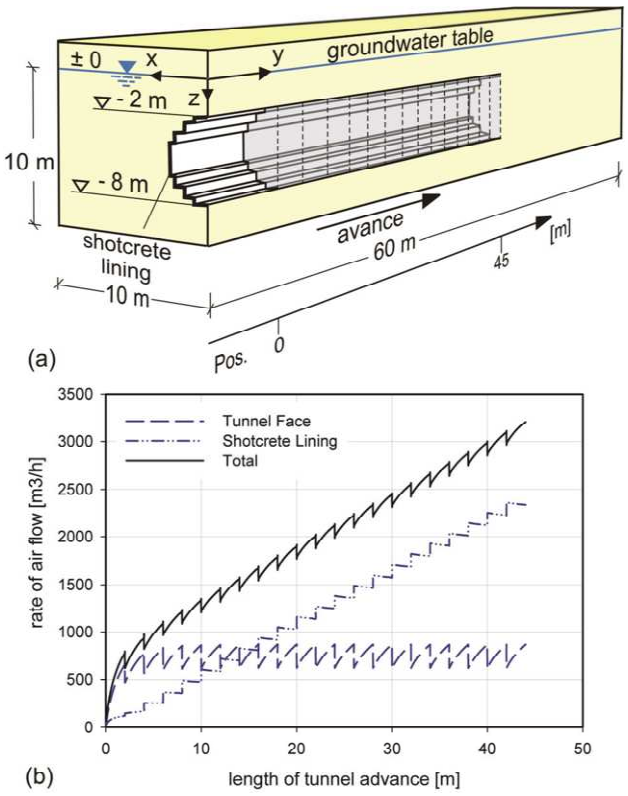

Figure 6. Geometry of the 3 dimensional tunnel advance model

REFERENCES

Arz, P.; Schmidt, H.G.; Seitz, J.; Semprich, S. 1994. Grundbau. Sonderdruck aus dem Betonkalender 1994, S. 165. Ernst & Sohn, Berlin.

van Genuchten, M.Th. 1980. A closed-form equation for predicting the hydraulic conductivity of unsaturated soils, *Soil Sci. Soc. Am. J.*, 44, 892-898.

Corey, A.T.1954. The Interrelationship between gas and oil relative permeabilities, *Procedures Montly*, 38-41.

Kammerer, G.; Semprich, S (2002). The Prediction of Air Loss in Tunnelling under Compressed Air. Felsbau 17, 1, 32-35.

Mualem, Y. 1976. A new model for predicting the hydraulic conductivity of unsaturated porous media, *Water Resour. Res.* 12, 513-522.

Pruess, K., Oldenberg, C. and Moridis, G. 1999. *TOUGH2 user's guide, version 2.0*, Earth Science Division, Ernest Orlando Lawrence Berkeley National Laboratory, University of California, 198p.

Poeter, E.P. and Hill, M.C. 1998. *Documentation of UCODE, A computer code for universal inverse modeling*, U.S. Geological Survey Water-Resources Investigations Report 98-4080, 116p.

Scheid, Y. 2003. Einfluss der Strömungsmechanik teilgesättigter Böden beim Tunnelbau unter Druckluft. Dissertation, Institut für Bodenmechanik und Grundbau, TU Graz (in print).

Steger, G. 2004. Implementierung der Vortriebssequenz in ein räumliches numerisches Modell eines Tunnelvortriebs unter Druck-luft zur Ermittlung von Luftströmungsvorgängen. Diplomarbeit, Institut für Bodenmechanik und Grundbau, TU Graz, 77p.